ORIGINAL PAPER

Premotor nonspiking neurons regulate coupling among motoneurons that innervate overlapping muscle fiber population

Mariano Julián Rodriguez ·
Carlos Bernardo Perez-Etchegoyen · **Lidia Szczupak**

Abstract Recent work indicated that co-activity of different motoneurons (MNs) in the leech can be regulated through a network that is centered on a pair of nonspiking (NS) neurons. Here, we investigate whether this effect generalizes to different types of MNs that display differential co-activity patterns in different motor behaviors: the dorsal longitudinal excitors DE-3 and the dorsal and ventral excitors MN-L. The data indicates that both motoneurons are coupled to the NS neurons through rectifying junctions that are activated when the motoneuron membrane potential becomes more negative than that of the NS, and that they exert an inhibitory synaptic potential on NS via a polysynaptic pathway. In addition, DE-3 and MN-L are linked by junctions that allow mutual excitation but the transmission of excitatory signals from MN-L to DE-3 depended on NS membrane potential. The results support the view that NS neurons can play a central role in orchestrating the co-activity of MNs during motor behaviors.

Keywords Electrical coupling · Motor circuits · Leech · Rectifying junctions · Nonspiking neuron

Introduction

Several evidences indicate that, although motor circuits are highly hierarchical structures, the lower levels in this hierarchy play an important role in shaping motor patterns (Bizzi et al. 2000; Fetz et al. 2000; Cattaert and Le Ray 2001); interactions between premotor interneurons and

M. J. Rodriguez · C. B. Perez-Etchegoyen · L. Szczupak (✉)
Dto de Fisiología, Biología Molecular y Celular,
FCEN-UBA, IFIBYNE-CONICET, Buenos Aires, Argentina
e-mail: szczupak@mail.retina.ar

motoneurons form "movement primitives" or "spinal modules" (in vertebrates) responsible for the basic movement patterns that compose a motor behavior.

Because of its relative simplicity, the leech has been an excellent organism to learn about the organization of motor circuits (Kristan et al. 2005). Two findings suggest that horizontal interactions among excitatory motoneurons (MNs) may play a complex role in shaping motor patterns: MNs show a high degree of coupling among themselves (Ort et al. 1974; Fan et al. 2005); and a pair of nonspiking (NS) premotor neurons are electrically coupled to all excitatory MNs through rectifying electrical junctions (active when NS membrane potential is more negative than the MN membrane potential) (Wadepuhl 1989; Rela and Szczupak 2007). Recent work indicated that co-activity of different MNs can be regulated through a network that is centered on the NS neurons (Rela and Szczupak 2003). In this network, MNs are connected to NS neurons through two parallel pathways: (1) the rectifying electrical coupling between MNs and NS; and (2) excitation of MNs evoke a chemically mediated inhibitory potential in NS neurons through a polysynaptic pathway. This connectivity enables NS neurons to regulate the co-activity between two specific motoneurons, the CV motoneurons that control circular ventral muscles and the AE motoneurons that control the erection of skin annuli (Rela and Szczupak 2003).

In the present work, we have investigated whether this network can be generalized to other motoneurons in the leech. Specifically, we chose two excitors of longitudinal muscles: the dorsal excitor cell DE-3 that controls dorsal longitudinal muscles and the MN-L motoneuron that excites both dorsal and ventral longitudinal muscles (Stuart 1970). The interest in these particular MNs resides in the differential pattern of activity displayed by them in two behaviors of the leech, swimming and shortening. When

leeches are touched in the front they retreat by shortening; when touched in the back they swim away (Kristan et al. 1982). In each segment, shortening involves the concomitant activation of all the longitudinal motor neurons while swimming results from the alternation of dorsal and ventral contractions. Thus, during shortening DE-3 and MN-L are co-activated (Shaw and Kristan 1995), while during swimming DE-3 is active during dorsal contraction but MN-L is inhibited throughout the whole episode because its activation would impair the dorsal-ventral wave (Ort et al. 1974).

The connection between DE-3 and MN-L was studied in the past and the results suggested that they are linked by a rectifying junction that is active only when the membrane potential of DE-3 is more negative than that of MN-L (Ort et al. 1974). Here, we review the connection between these two motoneurons to check the hypothesis that NS neurons could regulate the coupling among them. The results indicate that DE-3, MN-L and NS are connected by the same set of connections previously described for other motoneurons, that DE-3 and MN-L can mutually excite each other, and that NS neurons regulate the transmission of excitatory signals from DE-3 to MN-L.

Materials and methods

Biological preparation

Adult medicinal leeches (*Hirudo* sp.), weighing 2–5 g, were obtained from a commercial supplier (Leeches USA, Westbury, NY, USA) and maintained at 15°C in artificial pond water. The animals were not fed for at least 1 month prior to dissection.

The leech nervous system is composed of 21 midbody ganglia and head and tail brains. Each midbody ganglion innervates one body segment and contains all the corresponding sensory neurons and motoneurons (Muller et al. 1981). The motoneurons project their axons through specific contralateral peripheral nerves. In the present work, we focused our attention on motoneurons that excite dorsal longitudinal muscles, the dorsal excitor 3 (DE-3), and on motoneurons that excite both dorsal and ventral longitudinal muscles, the L motoneuron (MN-L), whose somata are located on the dorsal side of each midbody ganglion (Stuart 1970). The somata of the bilateral pair of NS neurons are located in the anterior lateral packets, on the ventral side, in position 151 of the ganglion map and can be readily recognized by their electrophysiological properties (Wadepuhl 1989; Rela and Szczupak 2003). When the motoneurons and the NS cells were recorded intracellularly in the same ganglion, we mounted it dorsal side up, the motoneurons were accessed on the surface of the ganglion and the NS cell was accessed penetrating with the microelectrode through the neuropile in the region where the NS cell soma is expected to be found.

The studies were performed using isolated single ganglia, and isolated 3-ganglia chains (typically, midbody ganglia 7–9) bathed in normal saline (in mM: 115 NaCl, 4 KCl, 1.8 CaCl$_2$, 1 MgSO$_4$, 10 Tris base, 10 glucose; pH 7.4), at room temperature (20–25°C). The sheath covering the ganglia used for intracellular recordings was removed. To block the synaptic transmission, we used a solution with a high Mg^{2+}/Ca^{2+} ratio (7 mM MgCl$_2$ and 1 mM CaCl$_2$) (Calvino et al. 2005). In this solution, the osmolarity was kept constant by reducing the NaCl concentration. The bathing solutions were applied through the perfusion system.

Electrophysiology

Intracellular somatic recordings were made with microelectrodes pulled from borosilicate capillary tubing (FHC, Brunswick, ME, USA), filled with a 3 M potassium acetate solution (resistance 20–40 MΩ). The electrodes were connected to an Axoclamp 2B amplifier (Axon Instruments; Union City, CA, USA) operating in the bridge mode (Figs. 1, 2, 3, 4, 5, 6) or in the discontinuous current clamp mode (Fig. 7), as indicated in the figure legends. Extracellular activity was recorded in peripheral nerves, using suction electrodes connected to a differential a.c. amplifier (Model 1700, AM-Systems, Inc; Carlsborg, WA, USA). The intra and extracellular recordings were digitized using a Digidata 1320 interface (Axon Instruments) and acquired using Clampex protocols (pClamp 9.2, Axon Instruments) at a sampling rate of 10 kHz.

All neurons recorded intracellularly were recognized by their soma location, their electrophysiological properties and, in addition, in the case of the motoneurons, by the relative amplitude of the spike waveform in extracellular recordings of specific nerves, matched one-to-one with the intracellular action potentials. The spikes of DE-3 and MN-L can be recorded in the contralateral dorsal-posterior (DP) nerve and, in addition, the MN-L spikes are the largest spikes in the first branch of DP nerve (DPb1) (Ort et al. 1974). The DE-3 and MN-L spikes in DP nerves were initially identified in simultaneous intra and extracellular recordings; thereafter the spikes were identified by the relative amplitude in the extracellular trace.

The membrane potential of NS (Vm$_{NS}$) is particularly variable, showing frequent excursions of several millivolts. Thus, when we state that Vm$_{NS}$ was set at a given value, it implies that it is in a ~10 mV range centered on that value.

Data analysis

The recordings were analyzed using commercial software (Clampfit 9.0 and Axograph 4.5, Axon Instruments). Curve
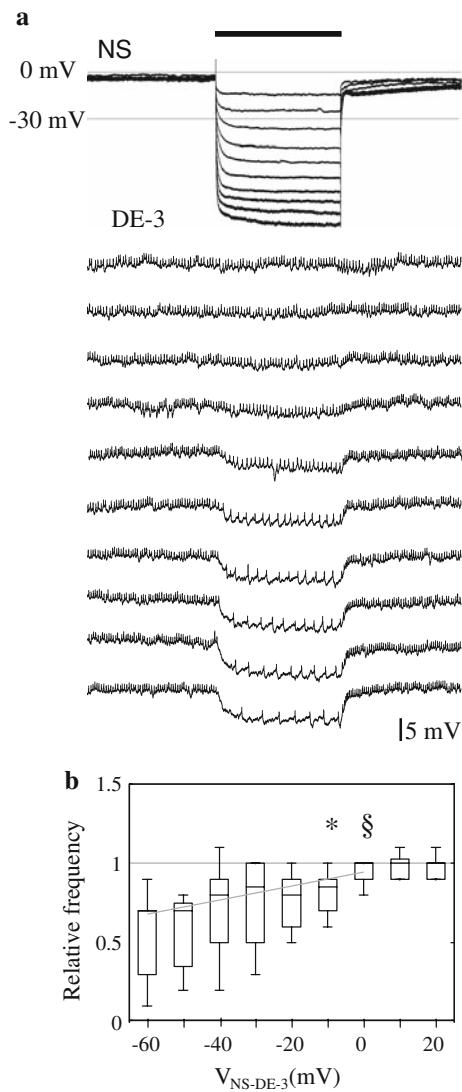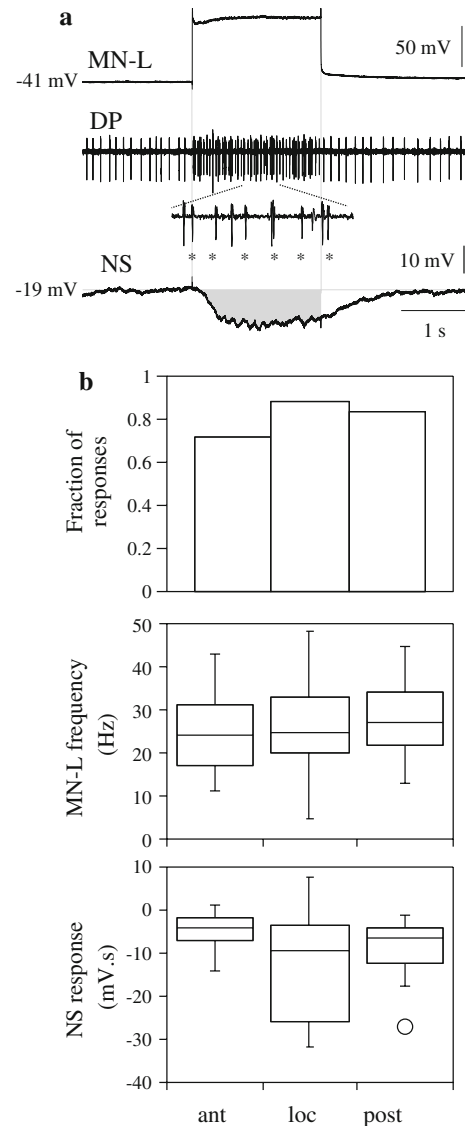
Fig. 1 Rectifying junction between NS neurons and DE-3 motoneurons. **a** Representative paired intracellular recordings of an NS neuron and a DE-3 motoneuron in which a series of 2-s square pulses of increasing amplitude were applied onto NS (from −0.5 to −5.0 nA, at 0.5 nA steps) at the time indicated by the *thick bar* on *top*. Extracellular recording of the contralateral DP nerve was performed but it is not shown. The experiment was performed with Vm_{DE-3} set at −30 mV while Vm_{NS} was set initially at 0 mV. *Horizontal dotted lines* on the NS recordings indicates 0 and −30 mV (where Vm_{NS} equals Vm_{DE-3} baseline). Paired recordings within a series are matched from *top* to *bottom*. The DE-3 spikes recorded at the soma are of small amplitude due to the passive invasion of fully developed action potentials initiated at an electrically distant site. **b** The *graph* shows Box–Whisker plots of the DE-3 firing frequency during the pulse relative to the frequency during a 2-s period prior to the pulse (relative frequency), as a function of the transjunctional potential $V_{NS–DE-3}$. The $V_{NS–DE-3}$ values ($n = 6$ pairs of cells) were grouped at 10 mV intervals. The *line* represents a linear fit for the median values in the range −60 to 0 mV ($R = 0.81$); *$P = 0.03$ and §$P = 0.06$ (one sample median Wilcoxon test with null hypothesis: the median of the corresponding bin equals one). At $Vm_{NS–DE-3}$ more negative than those marked by *asterisks* the relative firing frequency was significantly different from one ($P < 0.05$)
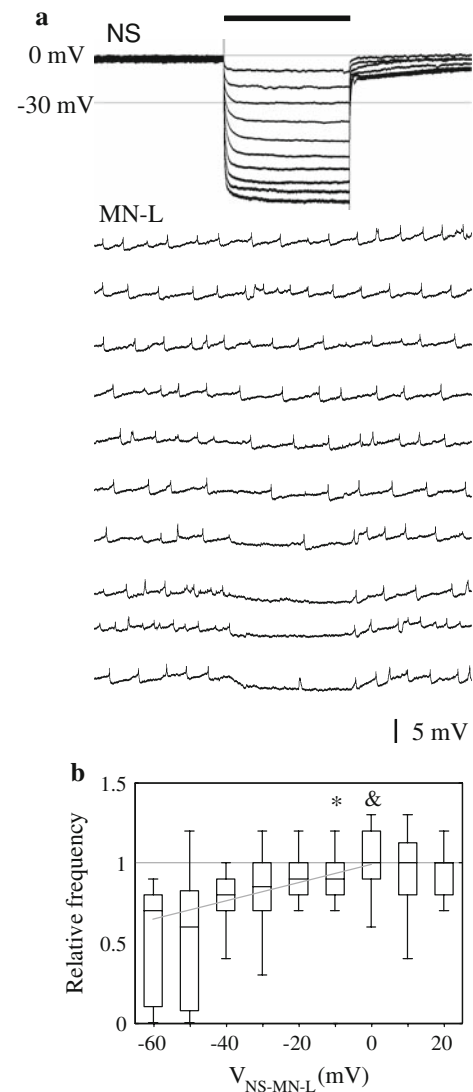
Fig. 2 Rectifying junction between NS neurons and MN-L motoneurons. **a** Representative paired recordings of an NS neuron and an MN-L motoneuron in which a series of hyperpolarizing square pulses of increasing amplitude were applied onto NS (from 0 to −8 nA, at 1 nA steps) at the time indicated by the *thick bar* on *top*. The experiment was performed with Vm_{MN-L} set at −30 mV while Vm_{NS} was set initially at 0 mV. *Horizontal dotted lines* on the NS recordings indicate 0 and −30 mV (where Vm_{NS} equals Vm_{DE-3} baseline). Paired recordings within a series are matched from *top* to *bottom*. The MN-L spikes recorded at the soma are of small amplitude due to the passive invasion of fully developed action potentials initiated at an electrically distant site. **b** The *graph* shows Box–Whisker plots of the MN-L relative firing frequency ($n = 9$ pairs of cells) as a function of the transjunctional potential $V_{NS–MN-L}$, measured during the current pulse. The Vm_{NS} values were grouped at 10 mV intervals. The *line* represents a linear fit for median values in the range −60 to 0 mV ($R = 0.84$). *$P = 0.04$ and &$P = 0.57$ (one sample median Wilcoxon test with null hypothesis: the median of the corresponding bin equals one). At $Vm_{NS–DE-3}$ more negative than those marked by *asterisks* the relative firing frequency was significantly different from one ($P < 0.05$)
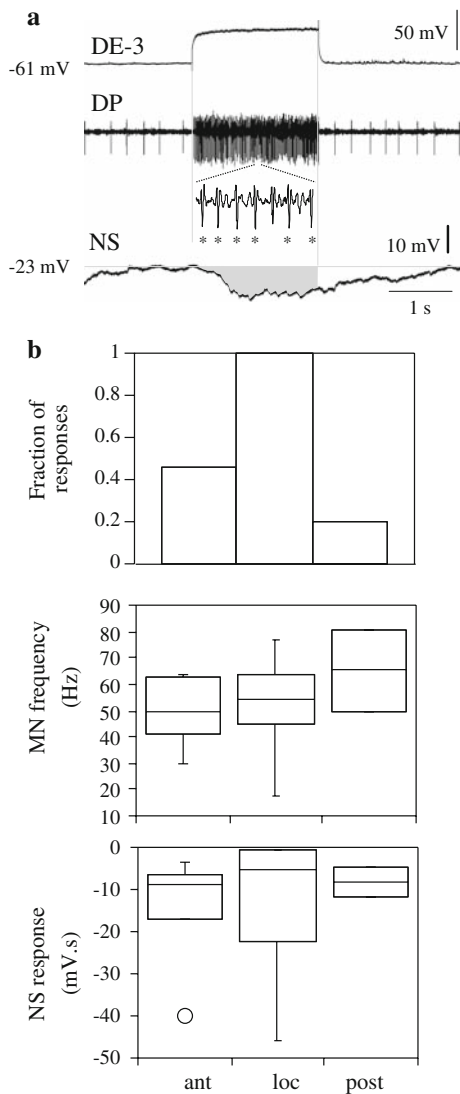
Fig. 3 Synaptic interaction between DE-3 motoneurons and NS neurons. **a** Representative paired intracellular recordings of a DE-3 motoneuron and an NS neuron and extracellular recording of a DP nerve (contralateral to DE-3) in the same ganglion. Square current pulses (1 nA, 2 s) applied to DE-3 motoneuron excited it. The DE-3 action potentials were identified in the DP nerve (see "Materials and methods") and the mean firing frequency during the pulse was calculated. Underneath the nerve recording an amplification of the trace shows that DE-3 spikes (marked with *asterisks*) that were sorted out from other spikes recorded in the DP nerve (mostly corresponding to MN-L motoneuron). DE-3 excitation evoked a hyperpolarizing response in NS neuron, set at around −20 mV. The *shaded area* represents the time integral of the response during the pulse. On the *left* of each intracellular trace, a reference membrane potential is indicated. **b** The *graphs* show, from *top* to *bottom*: the fraction of paired recordings in which the NS neurons showed a measurable response (>0.1 mV × s) (fraction of responses); Box–Whisker plots describing the firing frequency reached by the DE-3 motoneurons during the pulse; and Box–Whisker plots describing the mean time integral of the NS responses (excluding the non-responding ones). *Open circles* mark outliers. The results are sorted according to the relative location of DE-3 motoneuron with respect to NS neuron: in the adjacent anterior (ant, $n = 11$ pairs), same (loc, $n = 6$ pairs) and adjacent posterior (post, $n = 10$ pairs) ganglia
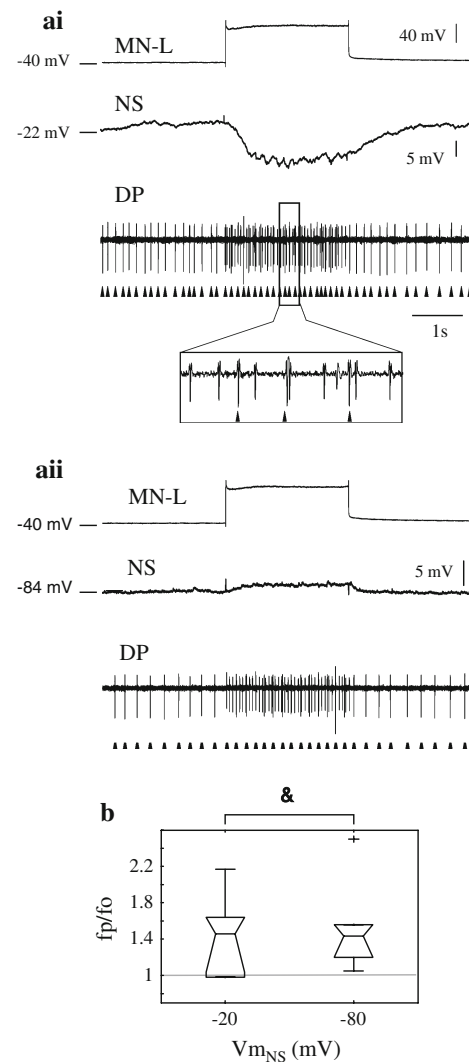
Fig. 4 Synaptic interaction between MN-L motoneurons and NS neurons. **a** Representative paired intracellular recordings of an MN-L motoneuron and an NS neuron and extracellular recording of a DP nerve (contralateral to MN-L) in a single ganglion. Square current pulses (4 nA, 2 ms) applied to MN-L motoneuron excited it. The MN-L action potentials were identified in the DP nerve (see "Materials and methods") and the mean firing frequency during the pulse was calculated. Underneath the recording an amplification of the trace shows that MN-L spikes (marked with *asterisks*) that were sorted out from other spikes recorded in the DP nerve (mostly corresponding to DE-3 motoneuron). MN-L excitation evoked a hyperpolarizing response in NS neuron, set at around −20 mV. The *shaded area* represents the time integral of the response during the pulse. On the *left* of each intracellular trace a reference membrane potential is indicated. **b** The *graphs* show, from *top* to *bottom*, the fraction of paired recordings in which the NS neurons showed a measurable response (>0.1 mV × s) (fraction of responses), Box–Whisker plots describing the firing frequency reached by the MN-L motoneurons and Box–Whisker plots describing the time integral of the NS responses (excluding the non-responding ones). *Open circles* mark outliers. The results are sorted according to the relative location of MN-L motoneuron with respect to NS neuron: in the adjacent anterior (ant, $n = 14$ pairs), same (loc, $n = 17$ pairs) and adjacent posterior (post, $n = 18$ pairs) ganglia
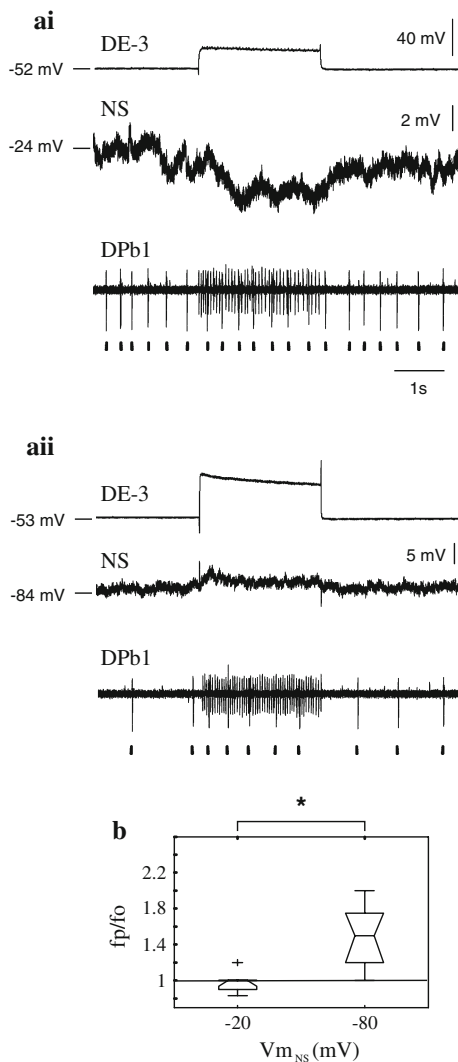
Fig. 5 Transmission of excitatory signals from DE-3 to MN-L depended on Vm_{NS}. **a** Paired intracellular recordings of an NS neuron and a DE-3 motoneuron and extracellular recording of a DPb1 nerve to monitor the MN-L firing frequency. The ticks underneath the recording indicate the MN-L spikes. The DE-3 motoneuron was stimulated (1 nA, 2 s) with a square current step while NS was set at around −20 mV (**ai**) or at around −80 mV (**aii**). On the *left* of each intracellular trace a reference membrane potential is indicated. **b** The Box–Whisker plot shows the change in frequency of the MN-L motoneuron during the injection of current in the DE-3 motoneuron, calculated as fp/f_0, where fp is the firing frequency during the pulse and f_0 is the basal firing frequency measured for 2 s prior to the stimulation step. The *graph* compares the data ($n = 7$ preparations) for the two conditions tested: Vm_{NS} at −20 and at −80 mV. *Asterisk* indicates $P = 0.04$ (Wilcoxon signed-rank test). The mean firing frequency (±SEM) of DE-3 upon stimulation with NS at −20 mV was 60 ± 11 Hz; and with NS at −80 mV was 41 ± 5 Hz. The mean basal firing frequency of MN-L (f_O) with NS at −20 mV was 4 ± 0.5 Hz and with NS at −80 mV was 2 ± 0.4 Hz

Fig. 6 Transmission of excitatory signals from MN-L to DE-3 did not depend on Vm_{NS}. **a** Paired intracellular recordings of an NS neuron and an MN-L motoneuron and extracellular recording of a DP nerve to monitor the DE-3 firing frequency. The *ticks* underneath the recording indicate the timing of the DE-3 spikes. Because in this recording DE-3 and MN-L spikes are of similar size we show an expanded view to confirm they can be distinguished. The MN-L motoneuron was stimulated with a square current step (4 nA, 2 s) while NS was set at around −20 mV (**ai**) or at around −80 mV (**aii**). On the *left* of each intracellular trace a reference membrane potential is indicated. **b** The Box–Whisker plot shows the change in frequency of the DE-3 motoneuron during the injection of current in the MN-L motoneuron, calculated as fp/f_0 (see Fig. 5). The *graph* compares the data ($n = 6$ preparations) for the two conditions tested: Vm_{NS} at −20 and at −80 mV. $^{\&}P = 0.75$ (Wilcoxon signed-rank test). The mean firing frequency (±SEM) of MN-L upon stimulation with NS at −20 mV was 16 ± 2 Hz; and with NS at −80 mV was 14 ± 2 Hz. The mean basal firing frequency of DE-3 (f_0) with NS at −20 mV was 9 ± 4 Hz and with NS at −80 mV was 6 ± 2 Hz

fitting was achieved using commercial software (Kaleidagraph 4.0, Abelbeck Software). Firing frequency was calculated by dividing the number of action potentials over a given lapse of time. Coupling coefficient was calculated as
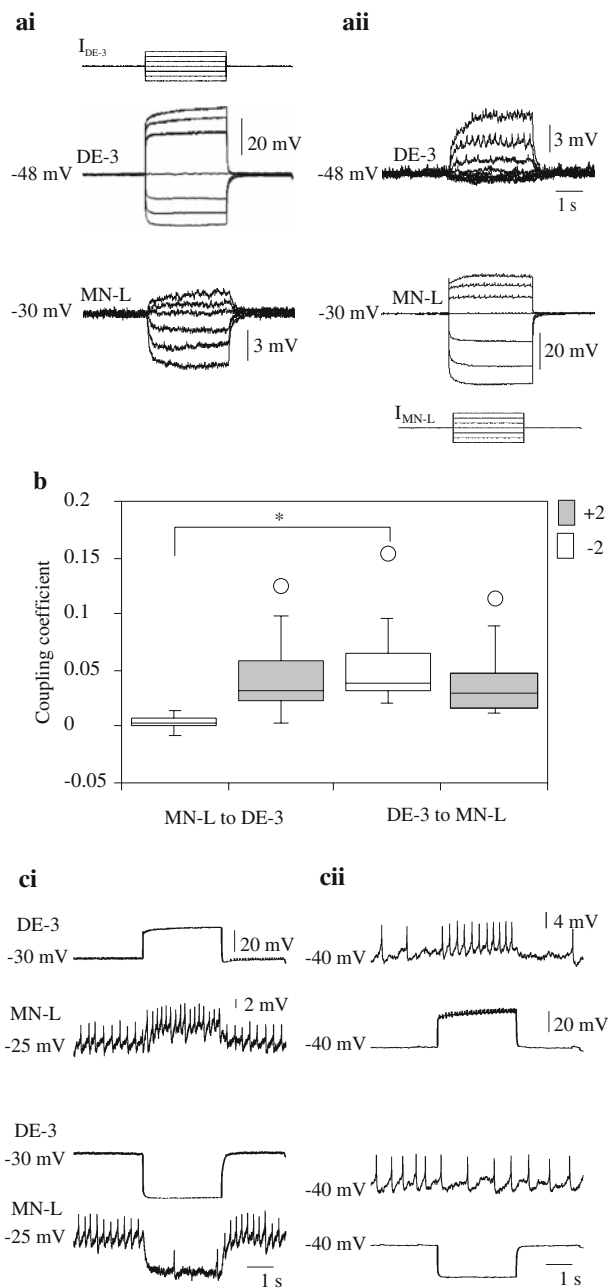
the change in membrane potential of the postsynaptic neuron over that of the presynaptic one.

Box–Whiskers plots indicate the median (horizontal solid lines in the boxes), the 25–75% (box) and the 10–90%

ai   **aii**

b

ci   **cii**

Fig. 7 Electrical coupling between DE-3 and MN-L. **a** Paired intra-cellular recording of motoneurons DE-3 and MN-L in a high Mg^{++} solution, as current step pulses (3 s) of increasing amplitude (-3 to $+3$ nA, at 1 nA steps) were injected in DE-3 (**ai**) and in MN-L (**aii**). Both paired traces were recorded in the same pair of cells. In these experiments the cell to which current was injected ("presynaptic cell") was recorded in discontinuous current clamp mode. On the *left* of each intracellular trace a reference membrane potential is indicated. **b** Box–Whisker plot describing the coupling coefficient measured in six ganglia in which DE-3 was stimulated (DE-3 to MN-L) and in 10 ganglia in which MN-L was stimulated (MN-L to DE-3) with pulses of $+2$ and -2 nA amplitude. *Asterisk* indicates $P = 0.001$ (Wilcoxon test). **c** Paired intracellular recording of motoneurons DE-3 and MN-L in a high Mg^{++} solution, as 3-s step pulses of $+2$ nA and -2 nA where injected in MN-L (**ci**) or in DE-3 (**cii**). The 'postsynaptic' motoneuron was set at a membrane potential at which it fired spontaneously

ranges (whiskers), and outliers (a value that is more than 1.5 times the interquartile range away from the limits of the box; open circles); number of neurons -or pairs of neurons-studied is expressed in parenthesis (*n*). Given that, in general, the data did not meet the assumptions for parametric tests (sample size, normality, equal variances), statistical significance of the differences was determined by non-parametric tests: Wilcoxon test for one sample (Figs. 1, 2) or paired samples (Figs. 5, 6, 7); Mann–Whitney for two independent samples (see "Results"); Kruskal–Wallis test for more than two independent samples (Figs. 3, 4) (Zar 1984). When more than one comparison was carried out using the same set of data (Fig. 7) the Dunn Sidak correction was performed (Sokal and Rohlf 1995).

Results

In the present study, we recorded NS neurons, whose soma is on the ventral face of midbody ganglia, through intracellular electrodes that approached from the dorsal face. The electrode traversed the ganglion at its anterior end, close to where the NS soma is expected to be located. NS neurons recorded in this way were identified by their characteristic spontaneous inhibitory synaptic potentials, the lack of classical fast spikes and the prolonged spike-like response caused on rebound from a deep hyperpolarizing pulse (Rela et al. 2009). The membrane potential of NS neurons thus recorded was of -45.3 ± 1.2 mV (mean $\pm$ SEM, $n = 7$) and showed an input resistance of 29.1 ± 4.3 MΩ (mean $\pm$ SEM, $n = 7$).

Electrical coupling between premotor NS neurons and motoneurons DE-3 and MN-L

Wadepuhl (1989) showed that motoneurons DE-3 and MN-L are coupled to NS neurons through rectifying electrical connections. With the aim of characterizing the activation threshold of these rectifying junctions, we performed simultaneous intracellular recordings of an NS neuron and a motoneuron in isolated ganglia. The membrane potential of NS (Vm_{NS}) was set at around 0 mV and that of the motoneuron (Vm_{MN}) was set at around -30 mV, at which it normally fires at a steady frequency. From this initial condition square current steps of negative current were injected in NS as we recorded the effect on the motoneurons. Given that the rectifying coupling between NS and the MNs is active at negative transjunctional potential ($Vj = Vm_{NS} - Vm_{MN}$) (Rela and Szczupak 2007), the initial conditions should set the NS–MN coupling at an inactive state. As the successive hyperperpolarizing pulses bring Vm_{NS} to more negative value, we expect to observe a change in the MN firing frequency. We chose to measure firing frequency rather than

Vm_{MN} deflection, because we considered the former a more sensitive variable than the latter (Rela and Szczupak 2007).

Figure 1a shows representative NS and DE-3 recordings that illustrate the experimental protocol. A series of 2-s current pulses of increasing amplitude (−0.5 to −5 nA) was injected in NS while DE-3 was recorded intracellularly. Small Vm_{NS} deflections produced no significant change in Vm_{DE-3} or firing frequency but larger NS deflections decreased the firing rate of the motoneuron and hyperpolarized Vm_{DE-3}. The graph in Fig. 1b summarizes the results obtained in this series of experiments, showing that a transjunctional potential ($Vm_{NS–DE-3} = Vm_{NS} − Vm_{DE-3}$) in between 0 and −10 mV was required to produce a statistically significant change in DE-3 firing frequency. Starting from this threshold $Vm_{NS–DE-3}$ the activity of the motoneuron was a linear function of the transjunctional potential suggesting that, once activated, the coupling acquired a stable value that was independent from $Vm_{NS–DE-3}$.

Figure 2 shows that the coupling between NS and MN-L followed a highly similar pattern. MN-L at −30 mV fires at a lower frequency than DE-3 (Mason and Kristan 1982), but the effective change in this motoneuron activity took place also at a $V_{NS–DE-3}$ within 0 and −10 mV.

Using the Vm deflections in the NS neurons and the motoneurons, we calculated the coupling coefficient as the ratio ΔVm_{MN} over ΔVm_{NS}. The median value of the NS–DE-3 coupling coefficient was of 0.04 ($n = 6$) and that of the NS–MN-L coupling coefficient was 0.01 ($n = 9$); these values were not significantly different among themselves ($P = 0.16$, Mann–Whitney U test).

Together with the previous data (Wadepuhl 1989) these results indicate that both DE-3 and MN-L are linked to NS via rectifying junctions activated at a Vj of around 0 mV.

Excitation of DE-3 and MN-L caused a hyperpolarizing response in NS

In addition to the electrical connection, excitatory motoneurons are connected with NS neurons via a polysynaptic chemical pathway: excitation of the motoneurons causes a hyperpolarizing response in NS (Wadepuhl 1989; Rela and Szczupak 2003). To characterize the responses evoked by DE-3 and MN-L, we excited these motoneurons and recorded NS set to −20 mV to amplify the hyperpolarizing response. The experiment was performed in chains of three ganglia where we could stimulate the motoneuron in the ganglion where we recorded NS or in the adjacent anterior and posterior ganglia. MNs do not extend arborization to adjacent ganglia but the interneuron(s) that mediates MN–NS chemical interactions does (Rela and Szczupak 2003) and, therefore, the signal delivered by the MNs can be recorded in NS neurons in adjacent ganglia.

Figure 3a presents representative recordings that show a substantial hyperpolarizing response in NS as DE-3 was stimulated. A square current pulse injected in DE-3 evoked a hyperpolarizing response that outlasted the stimulus. Because the stimulus impaired the detection of the small action potentials recorded in the soma (at a depolarized potential they become even smaller) we monitored the spike frequency of the motoneuron in extracellular recordings of the contralateral DP nerve, where both DE-3 and MN-L send axons that produce large spikes. The results are expressed as the fraction of NS neurons that responded to the motoneuron excitation and as the magnitude of the NS response, expressed as the time integral of Vm_{NS} during the stimulus. Figure 3b summarizes the data indicating that while all the DE-3 motoneurons tested evoked a response in the NS neurons of the same ganglion, only around 40% of the DE-3 neurons affected NS neurons in the anterior ganglion and 20% in the posterior ganglion, but the average magnitude of the responses were not statistically different among themselves ($P > 0.5$, Kruskal–Wallis test).

Figure 4a shows representative recordings indicating that excitation of MN-L also evoked a hyperpolarizing response in NS. Figure 4b indicates that MN-L evoked responses with similarly high probability in local, anterior and posterior ganglia and the amplitude of these responses were not statistically different among themselves ($P > 0.5$, Kruskal–Wallis test).

These results indicate that excitation of DE-3 and MN-L activates an interneuronal layer that can hyperpolarize NS neurons in at least three ganglia.

NS neurons modulate the coupling among DE-3 and MN-L

The data presented so far indicate that excitation of either DE-3 or MN-L evoke hyperpolarizing responses in NS, which could be transmitted back to the motoneurons through the rectifying junctions. To analyze how the hyperpolarizing response of NS to DE-3 and MN-L affected the cross-talk between them, we excited one motoneuron and recorded the response of the other motoneuron while shifting NS above and below the reversal potential of the hyperpolarizing response. This experimental maneuver, applied to electrically coupled motoneurons in the leech, showed that Vm_{NS} modulated their co-activity (Rela and Szczupak 2003).

Figure 5ai shows the response of MN-L to a current pulse injected in DE-3 when NS was set at around −24 mV. Vm_{MN-L} was set at a value that rendered a steady firing to evaluate both an increase or decrease in MN-L firing frequency. To better distinguish the MN-L spikes from the barrage of DE-3 spikes present in the DP nerve, we monitored MN-L spikes through extracellular recordings of the DPb1 nerve (Ort et al. 1974). Excitation of DE-3

caused a hyperpolarizing response in NS and no change in MN-L firing. Setting Vm_{NS} at −80 mV resulted in a reversed NS response to DE-3 excitation, and in this case MN-L firing frequency showed a substantial increase (Fig. 5aii). Figure 5b summarizes the results obtained in this series of experiments indicating that DE-3 excited MN-L when Vm_{NS} was set at −80 mV, but not when it was set at −20 mV. Note that shifting Vm_{NS} from −20 to −80 mV decreased MN-L firing frequency, as expected; however, this difference should not influence its ability to be excited as MN-L can fire well above the frequency recorded with NS at −20 mV (Mason and Kristan 1982).

When similar experiments were performed injecting current in MN-L and recording the response of DE-3, we found that the excitatory signal was transmitted from MN-L to DE-3 irrespective of the value at which Vm_{NS} was set (Fig. 6).

Motoneurons DE-3 and MN-L are electrically coupled

The results presented in Figs. 5 and 6 indicate that motoneurons DE-3 and MN-L can excite each other. To evaluate whether the mutual excitation is transmitted through direct electrical synapses between these motoneurons, we recorded both cells in the presence of a high Mg^{++} solution to avoid the influence of chemical interactions. Figure 7 shows representative recordings in one pair of DE-3 and MN-L motoneurons in which square current pulses (−2.5 to 2.5 nA, in 0.5 nA steps) were injected in DE-3 (Fig. 7ai) or in MN-L (Fig. 7aii). The results show that depolarizing pulses in DE-3 depolarized MN-L and vice versa. Noticeably, hyperpolarizing signals were transmitted from DE-3 to MN-L but hyperpolarizing signals evoked in MN-L were poorly transmitted to DE-3. Figure 7b summarizes the results for pulses of +2 and −2 nA injected in DE-3 or in MN-L. The results indicate that the coupling coefficient measured with the excitatory pulse was similar in both directions ($P > 0.5$, Wilcoxon test), while that measured with the inhibitory pulse was significantly smaller when the pulse was injected in MN-L ($P = 0.001$, Wilcoxon test).

To evaluate the effectiveness of the synaptic signals, we set the 'postsynaptic' neuron at a potential above threshold, at which the motoneurons fired at a low stead frequency. As it can be seen in the examples shown in Fig. 7ci depolarization of DE-3, although produced a small change in Vm_{MN-L}, increased the firing frequency of MN-L; and, as shown in Fig. 7cii, hyperpolarization of MN-L reduced the firing frequency of DE-3 in spite of the fact that it hardly affected the somatic recording of Vm_{DE-3}.

These results suggest that DE-3 and MN-L are electrically coupled through junctions that allow mutual excitation.

Discussion

The results presented contribute to the notion that motoneurons in the leech are linked by a wide web of electrical interactions. Electrical coupling among motoneurons has been observed both in invertebrates (Heitler 1978; Lotshaw and Lloyd 1990; Johnson and Hooper 1992; Norekian and Satterlie 1993) and vertebrates (Maeda et al. 1977; Perrins and Roberts 1995; Rekling and Feldman 1997; Kiehn and Tresch 2002).

Previous work in the leech nervous system revealed that besides coupling among bilateral pairs (Stuart 1970), different motoneurons that innervate the same muscle fibers are electrically coupled (Ort et al. 1974). In both cases, the coupling takes place through ohmic junctions. Here, we show that MNs that innervate overlapping but not identical muscle fibers were also electrically coupled and that this coupling could be partially modulated by the NS neurons (Fig. 5).

We interpret that this modulation can be exerted through the network of interactions described here. The scheme in Fig. 8 summarizes our interpretation: DE-3 and MN-L are electrically coupled among themselves via junctions that allow mutual excitation, and each one is connected to NS via rectifying junctions and via polysynaptic inhibitory synapses. The geometrical distances in the scheme represents hypothetical electrotonic distances and the asymmetry of the connectivity is proposed as an interpretation of the differential power of NS to modulate the co-activity between the motoneurons (Figs. 5, 6). When DE-3 is excited the signal follows two pathways towards MN-L: (1) it excites it via the electrical junction that links them directly and (2) it inhibits it indirectly through the inhibitory signal generated in NS that is transmitted to MN-L via the rectifying junction. The latter is only fully expressed when NS is depolarized and the two pathways balance each other. Notice that according to the model the hyperpolarizing signal was placed electrically close to the NS–MN-L junction. Differently, when MN-L is excited the inhibitory synapse onto NS is electrotonically distant from the NS–DE-3 junction, and therefore it lacks efficacy in counteracting the excitatory signal transmitted through the DE-3–MN-L junction.

When Vm_{NS} is at −80 mV, the hyperpolarizing synapse was close to its reversal potential and caused only a minor depolarizing change in Vm_{NS}. In this condition, there is a net excitatory signal through the DE-3–MN-L junctions, regardless of which is the stimulated motoneuron.

Ort et al. (1974) studied the interaction of DEs and VEs with motoneuron MN-L in normal saline and suggested that these motoneurons are linked through rectifying junctions that allow excitation to be transmitted only from MN-L to DE-3 and inhibition in the opposite direction. The results
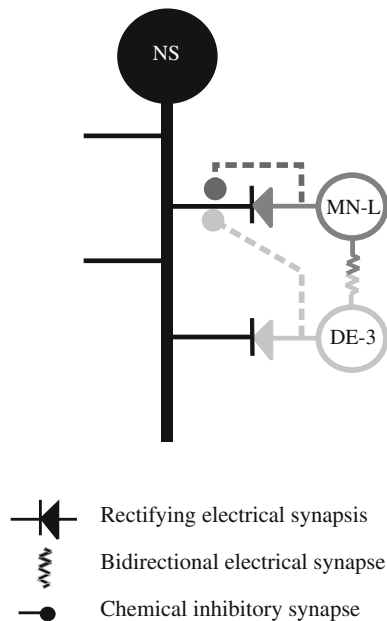
Fig. 8 Hypothetical connectivity diagram. The *diagram* represents NS neurons (*black*) extending branches that connect with MN-L (*dark gray*) and with DE-3 (*light gray*) through rectifying junctions. The motoneurons bear polysynaptic (represented by *broken lines*) inhibitory connections with NS, and are electrically coupled among themselves. Note that we used the resistor symbol for the latter, but this is not an ohmic resistance, but a bidirectional non-linear coupling. The relative distances between the connections imply electrical distances

presented here indicate that, provided that chemical interactions are minimized, DE-3 and MN-L can mutually excite each other. This does not contradict the observations made by Ort et al. who did not manipulate Vm_{NS}. Their observations are comparable to our results with NS at around −20 mV, in which MN-L excited DE-3 but DE-3 did not excite MN-L.

In the leech, spiking of different motoneurons was shown to be statistically independent (Arisi et al. 2001; Zoccolan et al. 2002). The coupling among motoneurons shown here, and in previous reports (Ort et al. 1974; Rela and Szczupak 2003), is relatively low and it is probably responsible for "dc equilibration" (Ort et al. 1974; Rela and Szczupak 2003), and not for firing synchrony. Leech muscles contract slowly and are poorly sensitive to the jitter of motoneuron spikes (Zoccolan et al. 2002) and, therefore, this low coupling level may well suit the co-activity necessary to produce the right motor output.

Future work should determine the relevance of the network centered on the NS neurons (Fig. 8) in the course of specific motor patterns. During swimming excitation of DEs and VEs takes place independent of each other, and they should not excite MN-L (Ort et al. 1974) since simultaneous dorsal and ventral contraction is incompatible with the swimming motor pattern; on the other hand during shortening excitation of MN-L occurs in conjunctions with excitation of

VEs and DEs (Shaw and Kristan 1995). If the circuit represented in Fig. 8 played a role in modulating the DE-3–MN-L coupling during swimming, one should expect that NS is depolarized during this motor behavior. In agreement with this expectation, NS neurons are depolarized during swimming, thus favoring an effective uncoupling of DE-3 and MN-L motoneurons (Rodriguez and Szczupak 2006), and preliminary data suggest that during shortening NS neurons are hyperpolarized, favoring the coactivity of the motoneurons. Therefore, it is possible that NS neurons contribute to set the motoneurons at the right level of co-activity to optimize the performance of the motor pattern.

References

Arisi I, Zoccolan D, Torre V (2001) Distributed motor pattern underlying whole-body shortening in the medicinal leech. J Neurophysiol 86:2475–2488

Bizzi E, Tresch MC, Saltiel P, dÁvella A (2000) New perspectives on spinal motor systems. Nature Rev Neurosci 1:101–108

Calvino MA, Iscla IR, Szczupak L (2005) Selective serotonin reuptake inhibitors induce spontaneous interneuronal activity in the leech nervous system. J Neurophysiol 93:2644–2655

Cattaert D, Le Ray D (2001) Adaptive motor control in crayfish. Prog Neurobiol 63:199–240

Fan RJ, Marin Burgin A, French KA, Friesen WO (2005) A dye mixture (Neurobiotin and Alexa 488) reveals extensive dye-coupling among neurons in leeches; physiology confirms the connections. J Comp Physiol A 191:1157–1171

Fetz EE, Perlmutter SI, Prut Y (2000) Functions of mammalian spinal interneurons during movement. Curr Opin Neurobiol 10:699–707

Heitler WJ (1978) Coupled motoneurones are part of the crayfish swimmeret central oscillator. Nature 275:231–234

Johnson MR, Hooper SL (1992) Overview of the stomatogastric nervous system. In: Harris-Warrick RM, Marder E, Selverston AI, Moulins M (eds) Dynamic biological networks. The stomatogastric nervous system. MIT Press, Cambridge

Kiehn O, Tresch MC (2002) Gap junctions and motor behavior. Trends Neurosci 25:108–115

Kristan WB, McGirr SJ, Simpson GV (1982) Behavioural and mechanosensory neurone responses to skin stimulation in leeches. J Exp Biol 96:143–160

Kristan WB Jr, Calabrese RL, Friesen WO (2005) Neuronal control of leech behavior. Prog Neurobiol 76:279–327

Lotshaw DP, Lloyd PE (1990) Peptidergic and serotonergic facilitation of a neuromuscular synapse in Aplysia. Brain Res 526:81–94

Maeda M, Magherini PC, Precht W (1977) Functional organization of vestibular and visual inputs to neck and forelimb motoneurons in the frog. J Neurophysiol 40:225–243

Mason A, Kristan WB (1982) Neuronal excitation, inhibition and modulation of leech longitudinal muscle. J Comp Physiol A 146:527–536

Muller KJ, Nicholls JG, Stent GS (1981) Neurobiology of the leech. Cold Spring Harbor Laboratory, Cold Spring Harbor

Norekian TP, Satterlie RA (1993) Cerebral neurons underlying prey capture movements in the pteropod mollusc, *Clione limacina*. I. Physiology, morphology. J Comp Physiol A 172:153–169

Ort CA, Kristan WB, Stent GS (1974) Neuronal control of swimming in the medicinal leech. J Comp Physiol A 94:121–154

Perrins R, Roberts A (1995) Cholinergic and electrical motoneuron-to-motoneuron synapses contribute to on-cycle excitation during swimming in *Xenopus* embryos. J Neurophysiol 73:1005–1012

Rekling JC, Feldman JL (1997) Bidirectional electrical coupling between inspiratory motoneurons in the newborn mouse nucleus ambiguus. J Neurophysiol 78:3508–3510

Rela L, Szczupak L (2003) Coactivation of motoneurons regulated by a network combining electrical and chemical synapses. J Neurosci 23:682–692

Rela L, Szczupak L (2007) In situ characterization of a rectifying electrical junction. J Neurophysiol 97:1405–1412

Rela L, Yang SM, Szczupak L (2009) Calcium spikes in a leech non-spiking neuron. J Comp Physiol A 195:139–150

Rodriguez MJ, Szczupak L (2006) A network of non-spiking premotor and spiking interneurons, connected by a funny array of chemical and electrical synapses, that selectively regulates motor pattern related motoneuron recruitment in a motoneuron activity dependent fashion. Annual Meeting of the Society for Neuroscience, Atlanta, GE

Shaw BK, Kristan WB (1995) The whole-body shortening reflex of the medicinal leech: motor pattern, sensory basis, and interneuronal pathways. J Comp Physiol A 177:667–681

Sokal RR, Rohlf FJ (1995) Biometry: the principals and practice of statistics in biological research, 3rd edn. W.H. Freeman and Company, San Francisco

Stuart AE (1970) Physiological and morphological properties of motoneurones in the central nervous system of the leech. J Physiol 209:627–646

Wadepuhl M (1989) Depression of excitatory motoneurones by a single neurone in the leech central nervous system. J Exp Biol 143:509–527

Zar JH (1984) Biostatistical analysis. Prentice Hall, Englewood Cliffs

Zoccolan D, Pinato G, Torre V (2002) Highly variable spike trains underlie reproducible sensorimotor responses in the medicinal leech. J Neurosci 22:10790–10800